Automatic region registration method based on spatially assistant plane

WANG Ruirui[1, 3], WANG Jinnian[1], YOU Hongjian[4], MA Jianwen[2]

1. *Institute of Remote Sensing Applications, Chinese Academy of Sciences, Beijing* 100101, *China*;
2. *Center for Earth Observation and Digital Earth, Chinese Academy of Sciences, Beijing* 100101, *China*;
3. *Graduate School of Chinese Academy of Sciences, Beijing* 100049, *China*;
4. *Institute of Electronics, Chinese Academy of Sciences, Beijing* 100080, *China*

Abstract: A new method of automatic region registration method based on spatially assistant planes is introduced in this paper. The method integrates both algorithm features of the global-region registration method's high precision and the local-region registration method's low complexity. Spatially assistant features with the same angle and resolution are calculated from, and the gray similarity is defined by normalized cross-correlation coefficient. By introducing the spatially assistant planes, spatially assistant features and gray similarity are combined together to register images. Two groups of images SPOT and ASTER, ASAR and ASTER, were tested. A mosaic was formed from the reference and re-sampled sensed images. In the mosaic, lineal features are well-aligned, which effectively proves that the automatic registration has a high accuracy.

Key words: spatially assistant plane, active and passive remote sensing images, automatic region registration, positive and negative function transforms, transform model

CLC number: TP751.1 **Document code:** A

Citation format: Wang R R, Wang J N, You H J and Ma J W. 2010. Automatic region registration method based on spatially assistant plane. *Journal of Remote Sensing*. **14**(3): 448—459

1 INTRODUCTION

Image registration is the process of aligning two or more than two images of the same scene acquired at different times, or from different angles, or by different sensors. Auto image registration is a core problem in computer vision and digital image processing, especially registration between images acquired with active and passive remote sensing sensors. Automatic registration has been widely used in image fusion (Moigne *et al*., 2006), change detection (Carlotto, 1997), medical image processing (Maintz & Viergever, 1998), map updating, etc. The accuracy of registration has a considerable influence on the usefulness of the final product. During the last three decades, many algorithms have been developed, which can be grouped into two categories: registration based on regions and registration based on features (Maintz & Viergever, 1998).

Automatic registration based on regions uses image digital number (DN) statistical information of regions to identify homologous points. The commonly used DN statistical values includes the sum of square intensity differences between the corresponding pixels, covariance, correlation coefficient (Inglada, 2002), normalized cross correlation coefficient (Kama *et al*., 2008), mutual information (Chen *et al*., 2003), grads (Shams *et al*., 2007), etc. Automatic registration based on regions is classified in two categories: (1) Registration based on local regions, the best value is found within a local region (Ardeshir *et al*., 1986). However, sometimes in the local region there is no matching point, which results in wrong registration. (2) Registration based on the global region, the best value is found within the global image (Wen *et al*., 2002). Its result has a high accuracy, although searching the wholly best value is a NP (Non-deterministic Polynomial) problem and has a highly computational complexity. Presently, automatic registration based on regions has been used successfully in aerial images (Lee *et al*., 1990), medical images (Shams *et al*., 2007); however, it does not make sense in the images which are lack of texture. Automatic regional registration is based on the pixel value of the image, and the registered result is not influenced by the density and accuracy of features. However, there are some disadvantages existing as follows: (1) it needs an amount of computations; (2) it depends on the image's gray statistical features excessively; (3) because of basing on gray similarity, it is adapted to registration between images with the same sensor. For the registration between images with different sensors, the result's accuracy becomes lower.

Received: 2009-03-17; **Accepted**: 2009-08-13

Foundation: National "863" High Technology Research and Development Program of China (No. 2007AA12Z157), Knowledge Innovation Program of the Chinese Academy of Sciences (No. O8S01100CX) and National Natural Science Foundation of China (No. 40901234).

First author biography: WANG Ruirui (1983—), female, PhD student, focuses on the research of artificial intelligent algorithms in remote sensing image processing.

In the method of automatic registration based on feature, the commonly used image features include point, line and plane which are robust to image noise. The image feature can also be classified as local or global features. Local features include point, boundary, line and small plane, and the global features include polygon, etc. Förstner (1986) and Hannah (1989) used points as local features to match images, Cross and Hancock (1995) used relation matching to process the global feature matching. The accuracy of automatic registration based on features depends on the accuracy of the identification of the features; in addition, much computing time is needed in the processing of picking out features. So the automatic registration based on feature adapts to images with dense or features which are distributed equally.

To overcome the drawbacks of the aforementioned two methods, recently some researchers have combined these approaches. Kim and Im (2003) first used an automated algorithm based on normalized cross correlation for the generation of control points (CPs) from the two images; Wen *et al*. (2008) combined spatial relations and organically feature similarity by introducing a function whose independent variable is the match matrix, which describes the correspondence of the features. But both the aforementioned two integrated methods are limited to registration between passive optical images.

This paper introduces a new method of automatic region registration based on spatially assistant plane, it adapts not only to registration between passive optical images, but also to registration between passive optical images and positive microwave images. The proposed method consists of four steps: (1) The positive and negative function transforms are used to construct two assistant planes which include spatial features with the same angle and resolution. (2) The small assistant plane is defined as the object window and the bigger one as searching window, and after automatic region searching, the corresponding feature points in the assistant planes are obtained. (3) The positive function transform is applied to obtain the corresponding feature points in the images. (4) Statistical analysis is carried out on all the feature points to select points with a high reliability to comprise the best feature point set. These points are used in a least square equation to generate the transform- ation model, with which, the sensed image is registered and the automatic registration is achieved.

2 AUTOMATIC REGION REGISTRATION METHOD BASED ON SPATIALLY ASSISTANT PLANE

Spatial features and gray similarity are combined together to register images by introducing spatially assistant planes. This method's flow chart is depicted as Fig. 1.

In the process of picking out spatially assistant planes' features, positive and negative function transforms are introduced. The approach is explained as follows: based on the image coordinates and geographical coordinates of the four boundary points in an image, the positive and negative function expressions

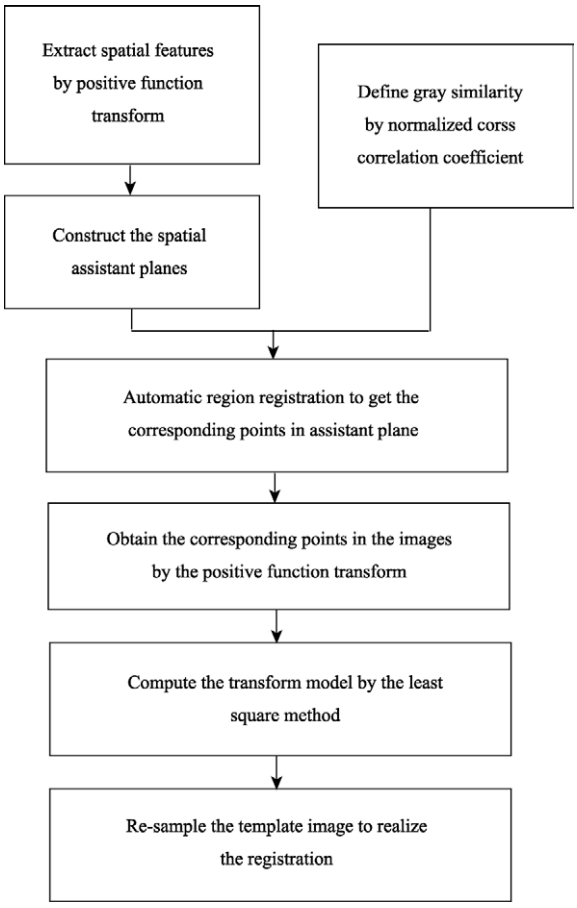

Fig. 1 Flow chart of automatic region registration method based on spatially assistant plane

can be constructed using an affine relation. The positive function computes the image coordinates of feature points from the corresponding geographical coordinates; and the negative function computes the geographical coordinates of feature points from the corresponding image coordinates.

2.1 Determine the features of spatially assistant planes by the positive and negative function transforms

This process is divided into three steps: (1) based on the image coordinates and geographical coordinates of the four boundary points in the reference and sensed images, the positive and negative function expressions of the reference and sensed images are constructed respectively. In addition, the reference image refers to the image to which the sensed image is aligned. (2) The feature points of the reference images are extracted in terms of the same spaces automatically, and their image coordinates are recorded. Based on the negative function transform, their corresponding geographical coordinates are obtained. (3) By defining the resolution of the reference image as the standard resolution, every feature point as the center, two groups of assistant planes are constructed. The information of every pixel in the assistant plane includes three aspects: plane coordinates, geographical coordinates and gray value.

The small plane has a same resolution as the reference image and 0°, and its size is fixed manually. Based on every feature point's geographical coordinates, the geographical coordinates of every pixel in the small assistant plane are obtained. By using the positive function transform, the corresponding reference image coordinates are obtained, and then processed by bilinear interpolation, every pixel's gray value within the plane is obtained from the reference images.

The larger plane's resolution and angle are identical to the small one, and its size is obtained based on the originally geographical error between the reference and sensed images. Every pixel's geographical coordinates and gray value are computed from the sensed image by the same method as the acquisition of every pixel's information in the small plane.

In Fig. 2, (a) is the small assistant plane; 101×101pixels, resolution 15m, gotten by positive function transformation and bilinear interpolation from the white-pane region in the (b); (c) is the bigger one, 201×201pixels, resolution 15m, gotten by positive function transformation and bilinear interpolation from the white-pane region in the (d).

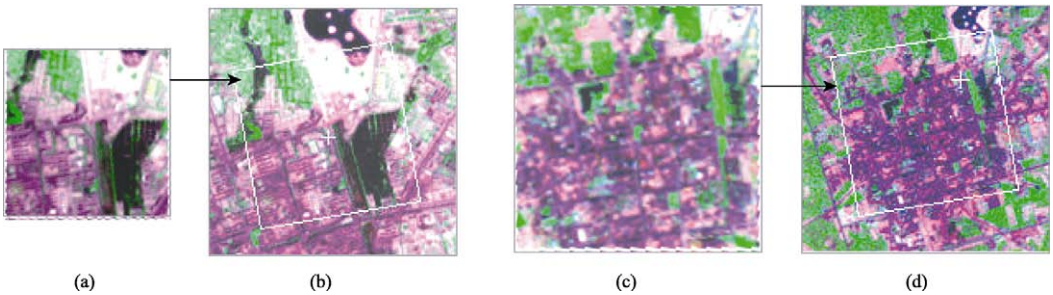

Fig. 2 The assistant planes of images

(a) small assistant plane, 101×101 pixels, resolution 15m; (b) reference image chip, the region in white rectangle is corresponding to (a), resolution 15m; (c) large assistant plane, 201×201 pixels, resolution 15m; (d) the sensed image chip, the region in white rectangle is corresponding to (c), resolution 30m; the positions of cross threads in (b) and (d) denote a couple of feature points

2.2 Automatic regional registration

Considering that the images are taken at different times, by different sensors or from different viewpoints, normalized cross-correlation coefficient is adopted as a similarity measure.

Normalized cross-correlation coefficient is a matching method based on statistical correlative theory. Firstly defining target window and searching window, when the target window is moved iteratively in the searching window, the gray values of the target window and the child window corresponding to the target window are inputted into target function (Eq. (1)), and then the normalized cross correlation coefficient is computed. The location with the highest value is the best matching location.

$$C(u,v)=\frac{\sum_x\sum_y[T(x,y)-\mu_T][I(x-u,y-v)-\mu_{I(u,v)}]}{\sqrt{\sum_x\sum_y[T(x,y)-\mu_T]^2\sum_x\sum_y[I(x,y)-\mu_{I(u,v)}]^2}} \quad (1)$$

In Eq. (1), $C(u,v)$ is normalized cross-correlation coefficient with a range [–1,1], x and y are the pixel coordinates in the target window, u and v are the offset values of the target window relative to the searching window, $T(x,y)$ is the DN value of the pixel in the reference image, $I(x,y)$ is the DN value of the pixel in the sensed image, μ_T is equal DN value of the target window, and μ_I is equal DN value of the sensed window.

After the gray feature is defined, the feature points could be searched by using of the two spatial assistant planes with a universal resolution and angle. The smaller of the spatially assistant planes is defined as the target window, and the larger one as the searching window. Based on the above-mentioned method, the corresponding feature points with geographical and plane coordinates are obtained.

2.3 Find the corresponding feature points by using the positive function transform

Based on the geographical coordinates of the feature points in the two assistant planes, the corresponding reference and sensed image coordinates are obtained by the reference and sensed images' respective positive function transforms. In Fig. 2, the positions of cross threads (b) and (d) denote a couple of feature points.

2.4 Image registration

Considering that not all the corresponding feature points are correct points, after the statistical analysis on the entire feature point set, the false points are removed, and the points with a high reliability are selected to comprise the best feature point set. The transform model (Eq. (2)) is obtained after inputting the best point set into the least square equation (Ackermann, 1983).

$$\begin{bmatrix}x'\\y'\end{bmatrix}=\lambda\begin{bmatrix}a_1 & a_2\\b_1 & b_2\end{bmatrix}\begin{bmatrix}x\\y\end{bmatrix}+\begin{bmatrix}\Delta x\\\Delta y\end{bmatrix}. \quad (2)$$

where λ is scale value, a_i, b_i (i = 1,2) are the oriented cosines formed by the angle function rotation angles, $[\Delta x\ \Delta y]^{\mathrm{T}}$ is translation vector, $[x\ \ y]^{\mathrm{T}}$ is the coordinates in the sensed image, and $[x'\ y']^{\mathrm{T}}$ is the coordinates after registration. After linearizing Eq. (2), the error equation and normal equation are obtained. The

transform model's parameters are obtained by computing the above equations. With the help of this model, the sensed image is registered and the automatic registration of images is achieved.

3 EXPERIMENTATION AND ANALYSIS

To validate the feasibility of this algorithm, two pairs of images, comprising ASTER and SPOT, ASAR and ASTER were used as experiments.

3.1 Registration of SPOT and ASTER images

SPOT and ASTER images covering the city of Zhangye town, Gansu Provience, China were registered (Fig. 3). The SPOT image was defined as the reference image, and the ASTER image as the sensed image. In the SPOT image, feature points were picked out automatically with a distance 101 pixels from each other in the northern and eastern orientation. By defining a feature point as the center, the corresponding small assistant plane was constructed with a size of 101×101 pixels; based on the original geographical error between SPOT and ASTER images, the large plane was constructed with a size of 201×201 pixels. After applying the algorithm introduced in this paper, 256 couples of feature points were obtained. Fig. 4 was the normalized cross correlation coefficient for all the feature points.

The SPOT and ASTER images were acquired at different times and by different sensors, thus the feature points' normalized cross correlation coefficients tend to be low. After much experimentation, the smallest threshold of normalized cross correlation coefficient is 0.3, which means that the feature points with a coefficient bigger than 0.3 are correct common points, while the others with a coefficient smaller than 0.3 are not. The best feature point set was formed by the feature points with a coefficient greater than 0.6.

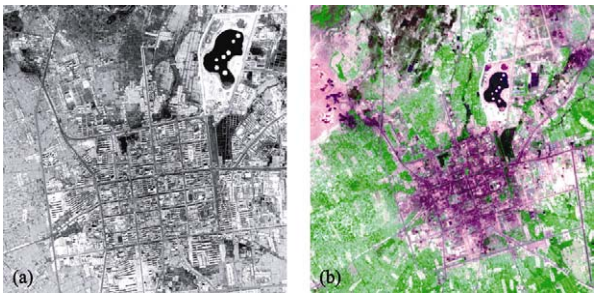

Fig. 3 Original experimental images of SPOT and ASTER images (Zhangye town, Gansu province)
(a) SPOT image(pan band), taken on March 29th, 2008, 2000×2000 pixels, resolution 2.5m, angle 0°, defined as reference image; (b) ASTER image (2,3,1 bands), taken on May 23rd, 2008, 500×500 pixels, resolution 15m, angle 10.3862°, defined as template image

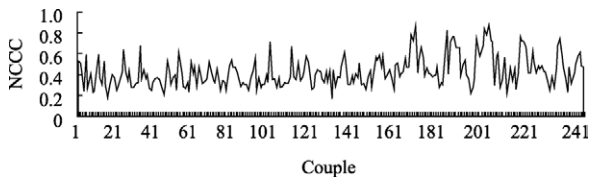

Fig. 4 Distributing plot of normalized cross-correlation coefficient (NCCC) for SPOT and ASTER images

Fig. 4 is the result images after registration. Fig. 5(a) is the registered ASTER image with a same angle and resolution as SPOT image. In order to display the accuracy of registration, the different parts of SPOT image and registered ASTER image are picked up to build a new image which is depicted as Fig. 5(b), from the left, SPOT and registered ASTER image are respectively displayed. By comparing to the original ASTER image (Fig. 3(a)), it is indicated that every kind of objects and texture is smooth and natural in the intersecting place, which effectively proved that the registration result has a high accuracy.

3.2 Registration of ASAR and ASTER images

ASAR and ASTER images covering the city of Beijing, China were registered (Fig. 6). ASAR image was defined as the reference image, and ASTER image as the sensed image. In the ASAR image, every feature point was picked out automatically

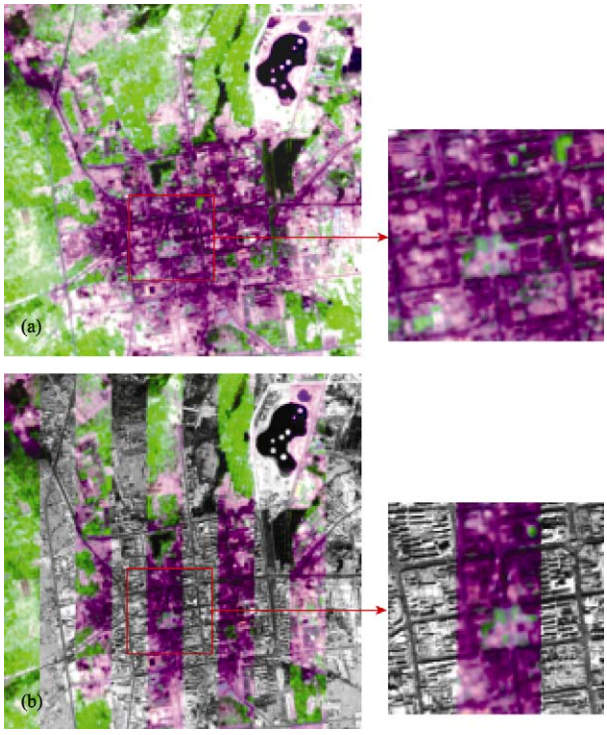

Fig. 5 Registration resulting images of SPOT and ASTER images
(a) registered ASTER image and local room figure, with the same angle and resolution as SPOT image; (b) Mosaic image and the local room figure, which is obtained by picking up the different trips of SPOT and registered ASTER images, from the left, registered ASTER and SPOT images are respectively displayed

with a distance 101 pixels from each other in the northern and eastern orientation. The small assistant plane's size was fixed as 101×101 pixels; based on the geographical error between ASAR and ASTER images, the other plane was constructed with a size of 201×201 pixels. After processed by the algorithm introduced in this paper, 81 couple feature points are gotten. Fig. 7 is the distributing chart of all the feature points' normalized cross correlation coefficient.

ASAR image is SAR (synthetic aperture radar) image, whose value is the back scattering energy of objects; while TM is optical image, whose value is the reflected or emissive radiant energy of objects. The imaging mechanism between them is different which results in that all feature points' normalized cross correlation coefficients are wholly lower. After much experimentation, the smallest threshold of normalized cross correlation coefficient is 0.2. The best feature point set is formed by the feature points with a coefficient bigger than 0.25.

Fig. 8 is the result images after registration. Fig. 8(a) is the registered ASTER image with a same angle and resolution as ASAR image. Fig. 8(b) is a new image which is built by picking up the different parts of ASAR image and registered ASTER image. By comparing to the original ASAR image (Fig. 6(a)), it is indicated that every kind of object such as roads, rivers and buildings is smooth and natural in the intersecting place, which effectively proved that the registration result has a high accuracy.

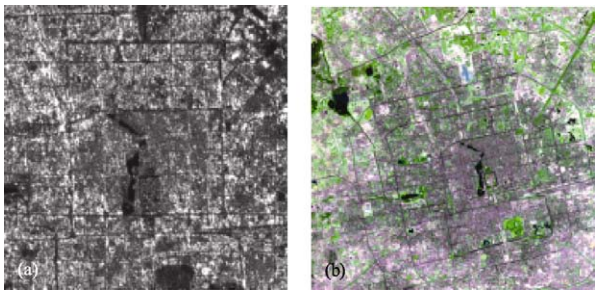

Fig. 6 Original experimental images of ASAR image and ASTER image (Beijing City)

(a) ASAR image (HH polarized), taken on April 27th, 2004, 1000×1000 pixels, resolution12.5m, angle 0°, defined as reference image; (b) ASTER image (2,3,1 bands), taken on April 9th, 2004, 1500×1500 pixels, resolution 15m, angle 10.3862°, defined as template image

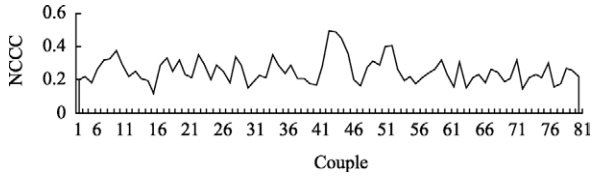

Fig. 7 Distributing plot of normalized cross-correlation coefficient (NCCC) for ASAR image and ASTER image

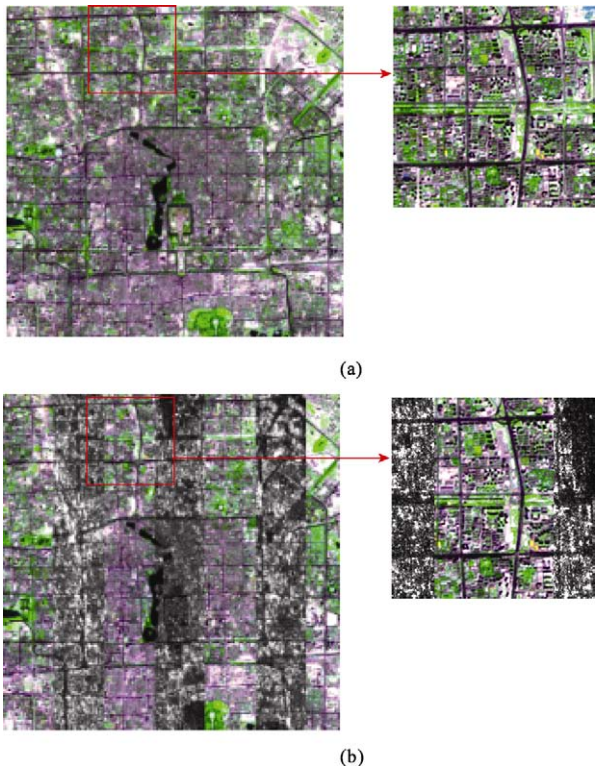

Fig. 8 Registration result images of ASAR image and ASTER image

(a) Registered ASTER image obtained by automatic region registration method based on spatial assistant plane, with the same angle and scale as the reference image; (b) Mosaic image obtained by picked up the different trips of Registered ASTER image and ASAR image, from the left, Registered ASTER image and ASAR image are respectively displayed

4 CONCLUSION

Aiming at the problem in the active and positive remote sensing images' registration, this paper brings forward a new method of automatic region registration based on spatial assistant plane, which combines spatially assistant plane's feature and gray feature. This algorithm is not only of high accuracy which is similar to the registration based on the whole region, but also of a lower computational complexity and quick speed because that the searching of feature points is limited in the assistant plane with spatially consistent features, not in the whole image region. This algorithm is adapted to images which have big difference in angle and resolution between them. In addition, by using of the normalized cross correlation coefficient to define the gray similarity, the influence of the difference between images' tone on registration result is reduced, which makes the algorithm more robust.

REFERENCES

Ackermann F. 1983. High precision digital image correlation. Proceeding of the 39th Photogrammetric Week

Ardeshir G, George C S and Carl V P. 1986. A region-based approach to digital image registration with subpixel accuracy. *IEEE Transactions on Geoscience and Remote Sensing*, **24**(3): 390—399

Ayaehe N and Fvaerjon B.1985. Fast setero matching of edge segments using prediction and verifi-ceation of hypotheses. Proceedings of Computer Vision and Pattern Cognition

Brown L G. 1992. A survey of image registration techniques. *ACM Computing Survey*, **24**(4): 325—376

Carlotto M J. 1997. Detection and analysis of change in remotely-sensed imagery with application to wide area surveillance. *IEEE Transactions on Image Processing*, **6**(1): 189—202

Chen H, Varshney P and Arora M. 2003. Performance of mutual information similarity measure for registration of multitemporal remote sensing images. *IEEE Transaction on Geoscience and Remote Senseing*, **41**(11): 2445—2454

Förstner W. 1986. A feature based correspondence algorithm for image matching. *International Archives of Photogrammetry and Remote Sensing*, **26**(3): 150—166

Hannah M J. 1989. A system for digital stereo image matching. *Photogrammetric Engineering and Remote Sensing*, **55**(12): 1765—1770

Inglada J. 2002. Similarity measures for multisensor remote sensing images. International Geoscience and Remote Sensing Symposium (IGARSS)

Karna D K, Agarwal S and Nikam S. 2008. Normalized cross-correlation based fingerprint matching. 2008 Fifth International Conference on Computer Graphics, Imaging and Visualisation

Kim T and Im Y. 2003. Automatic satellite image registration by combination of matching and random sample consensus. *IEEE Transaction on Geoscience Remote Sensing*, **41**(5): 1111—1117

Lee H J and Lei W L. 1990. Region matching and depth finding for 3-D objects in stereo aerial photographs. *Pattern Recognition*, **23**(2): 81—93

Maintz J B A and Viergever M A. 1998. A survey of medical image registration. *Medical Image Analysis*, **2**(1): 1—36

Moigne Le, Cole-Rhodes J, Eastman A, Jain R, Joashua P, Memaradeghi A, Mount N, Netanyahu D, Morisette N and Uko-Ozore J. 2006. Image registration and fusion studies for the integration of multiple remote sensing data. International Geoscience and Remote Sensing Symposium 2006 (IGARSS'06)

Shams R, Kennedy R A, Sadeghi P and Hartley R. 2007. Gradient intensity-based registration of multi-modal images of the brain. IEEE 11th International Conference on Computer Vision(ICCV 2007)

Wen G, Li D and Yuan X. 2002. A global optimal registration method for satellite remote sensing images. Proceedings ISPRS Commission III Symposium

Wen G, Lu J and Yu W. 2008. A high-performance feature-matching method for image registration by combining spatial and similarity information. *IEEE Transactions on Geoscience and Remote Sensing*, **46**(4): 1266—1277

Vosselman G. 1992. Relational matching. Springer, Berlin: Lecture Notes in Computer Science

Zhao F, Huang Z and Gao W. 2006. Image matching by normalized cross-correlation. International Conference on Acoustics, Speech and Signal Processing 2006(ICASS'06)

结合空间辅助面特征的区域自动配准

王瑞瑞[1,3], 王晋年[1], 尤红建[4], 马建文[2]

1.中国科学院 遥感应用研究所, 北京 100101;
2.中国科学院 对地观测与数字地球科学中心, 北京 100101;
3.中国科学院 研究生院, 北京 100049;
4.中国科学院 电子学研究所, 北京 100080

摘 要: 提出了一种新的基于空间辅助面特征的主被动遥感影像区域自动配准方法, 该方法借鉴了全局区域配准高精度与局部区域配准低复杂度的算法特征, 采用正、反函数变换法提取具有相同角度和尺度的空间特征, 并采用归一化互相关系数法定义灰度相似性, 通过构建空间辅助面, 将空间特征和灰度相似性有效地结合起来, 共同用于影像的自动配准。文中选取了 SPOT 与 ASTER 影像、ASAR 和 ASTER 影像两组数据进行实验, 并提取基准影像和配准后待配准影像的不同部位相间拼接形成结果图, 从中可以看出各种地物在拼接处表现自然平滑。实验结果证明, 该方法简单易行, 且配准精度较高。

关键词: 空间辅助面特征, 主被动遥感影像, 区域自动配准, 正、反函数变换, 变换模型

中图分类号: TP751.1 文献标识码: A

引用格式: 王瑞瑞, 王晋年, 尤红建, 马建文. 2010. 结合空间辅助面特征的区域自动配准. 遥感学报, **14**(3): 448—459
Wang R R, Wang J N, You H J and Ma J W. 2010. Automatic region registration method based on spatially assistant pane. *Journal of Remote Sensing*. **14**(3): 448—459

1 引 言

影像自动配准是计算机视觉以及数字图像处理的基本问题, 尤其是主被动遥感影像的自动配准, 它在影像融合(Moigne 等,2006)、变换检测(Carlotto,1997)、环境检测、医学图像处理(Maintz and Viergever,1998)以及地图更新等方面有着广泛的应用, 影像配准的精度在很大程度上影响着后续处理的结果。近年来许多学者对其进行了深入的研究, 提出了各种用于自动配准的方法, 主要分为两类: 基于区域的自动配准和基于特征的自动配准(Maintz & Viergever,1998)。

基于区域的自动配准主要是利用了一定区域中灰度的统计特征信息来识别同名点, 通常使用的灰度统计信息包括对应像元的平方差、协方差、差的平方和、相关系数(Inglada,2002)、互相关系数(Karna 等, 2008)、互信息(Chen 等, 2003)、梯度(Shams 等, 2007)等。基于区域的自动配准可以分成两种: (1)基于局部区域的自动配准。主要是从需要匹配点的特定邻域内获得对于该点的匹配支持, 从而寻求局部最优的解(Ardeshir 等, 1986)。由于只是从局部考虑问题, 所以容易造成错误的配准; (2)基于全局区域的自动配准。从全局最优的方式考虑问题, 把配准看作一个寻求全局能量函数最小的过程, 从而获取全局最优的结果(Wen 等, 2002)。该方法具有结果准确度高的优点; 但是寻求全局最优解是一个 NP-Hard 问题, 它需要耗费大量的计算时间。目前, 基于区域的配准方法已经被成功的应用于航天图像(Lee 等, 1990)、医疗图像(Shams 等, 2007)。对于缺乏纹理特征的图像, 或者在图像的边界不连续区域, 这种方法将变得没有意义(Ayaehe & Fvaerjon, 1985)。基于区域的自动配准法直接对图像像元进行配准, 结果不受特征提取精度和密度的影响, 可得到较高的定位精度; 同时它也存在着以下弊端: (1)需要进行大量的计算和比较, (2)过于依赖图像灰度统计特性, (3)该方法基于像元的灰度特性进行配准, 所以

收稿日期: 2009-03-17; 修订日期: 2009-08-13

基金项目:863 计划(编号: 2007AA12Z157)、中国科学院知识创新工程青年人才领域前沿项目专项项目(编号: O8S01100CX)和国家自然科学基金项目(编号: 40901234)。

第一作者简介: 王瑞瑞(1983—), 女, 河南焦作人, 博士研究生, 主要研究方向为数字图像智能处理。

适用于同一传感器影像的配准，对于不同传感器的影像或者同一传感器的时差偏大的影像，配准结果较差。

基于特征的配准，主要分为 3 个步骤：(1)特征提取；(2)利用一组参数对特征进行描述；(3)利用参数进行特征配准。常用的图像特征包括点、线、面。通常情况下，提取的特征比较明显，能够抵抗噪声的干扰(Förstner, 1986)。图像特征又分为局部特征和全局特征两类：局部特征包括点、边缘、线条和小的区域，全局特征由一些局部特征组成，比如多边形。Förstner(1986), Hannah(1989)选取特征点作为局部特征进行影像匹配。Vosselman(1992)利用关系匹配处理全局特征的匹配。与基于区域的配准方法相比，特征受几何变形和辐射差异的影响较小，配准的结果更加精确；但是配准精度依赖于特征提取的精度，且特征提取的计算量大，需要预先指定一些参数或者阈值。因此基于特征的配准法适用于特征密集或者分布均匀的影像，对于特征稀疏以及特征分布不均衡的影像配准结果较差。

为了克服以上两大类方法的弊端，近年来一些研究者将两种方法结合起来，取得了一定的成果。Kim 和 Im(2003) 基于归一化互相关系数法对两幅图像中的控制点进行配准, Wen 等(2008)通过建立一个函数将空间关系和特征相似结合起来，该函数的独立变量就是匹配矩阵，通过求解该函数的最大值寻找配准的最佳特征点。以上两种算法只局限于被动光学图像之间的配准。

本文提出了一种新的结合空间辅助面特征的区域自动配准方法，同时适用于被动光学图像之间、被动光学图像和主动微波图像之间的配准。具体配准的流程分为 4 步：(1)利用正、反函数变换消除两幅影像在角度和尺度上的差异，提取空间辅助面特征，构建大小两个辅助面；(2)将小辅助面作为目标窗口，大辅助面作为搜索窗口，采用区域配准法进行搜索，获取辅助面中的同名特征点；(3)利用正函数变换得到配准影像中的同名特征点；(4)对配准后的同名特征点结果进行统计分析，选取可靠性高的特征点组成最佳特征点集，代入最小二乘法求解得变换模型，利用该模型对待配准影像进行重采样，实现两幅影像的自动配准。

2 结合空间辅助面特征的区域自动配准方法

结合空间辅助面特征的区域自动配准方法通过构建空间辅助面，将影像的空间特征和灰度特征结合了起来，共同用于影像的配准。该方法的流程如图 1。

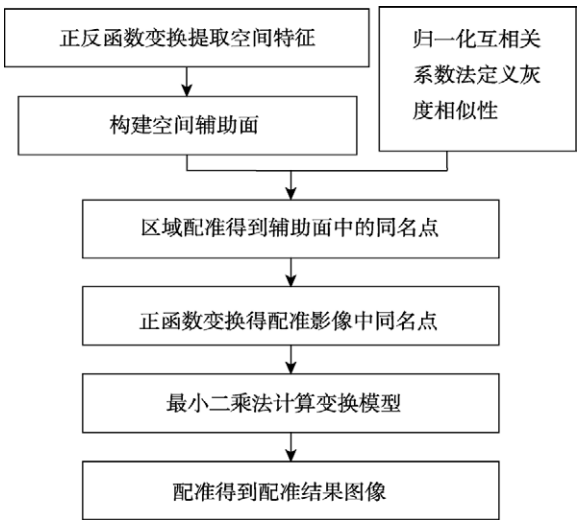

图 1　基于空间辅助面特征的区域自动配准法流程图

在结合空间辅助面特征的区域配准法中，本文采用正反函数变换法提取具有相同角度和尺度的空间辅助面特征。正反函数变换法的基本思想为：利用影像 4 个边界点行列坐标及其地理坐标信息，求取影像行列值和地理坐标值之间的仿射关系，构建正反函数的关系表达式。其中，正函数表达式是根据像点的地理坐标值求解对应的行列坐标值，反函数表达式是根据像点的行列坐标值求解对应的地理坐标值。

2.1　正、反函数变换提取空间辅助面特征

正函数变换提取具有相同角度和尺度的空间辅助面特征，主要分为以下 3 个步骤：(1)利用基准影像和待配准影像 4 个边界点行列坐标值和地理坐标值，分别构建基准影像和待配准影像的正反函数表达式；(2)提取基准影像中的特征点，记录对应的行列坐标值，根据反函数表达式，得到特征点的地理坐标值，在本文中，基准影像中的特征点是人为设定的；(3)以基准影像像元尺寸为大小，以基准影像中每个特征点为中心，构建大小不一两个辅助面。辅助面中每个像元点的信息包括 3 个方面：行列坐标值，地理坐标值和灰度值。

小辅助面的大小可以人为设定，尺度与基准影像相同，设定角度偏差为 0。根据小辅助面中心特征点的地理坐标值，得到所有像元点的地理坐标值。像元点灰度值的获取分为两步：根据小辅助面中每

个像元点的地理坐标，通过基准影像的正函数表达式计算，得到像元点在基准影像中对应的行列坐标值，然后采用双线性内插公式重采样，获取小辅助面中每个像元点的灰度值。

大辅助面的大小根据基准影像和待配准影像之间的地理坐标偏差设定，尺度与基准影像相同，设定角度偏差为 0，采用与获取小辅助面中像元点地理坐标值和灰度值相同的方法，得到大辅助面中像元点的地理坐标值和灰度值。

如图 2，(a)为小辅助面，大小为 101×101 像元，分辨率为 15m；是根据基准影像片(b)中白色方框里的区域，通过正反函数表达式和双线性内插公式得到；(c)为大辅助面，大小为 201×201 像元，分辨率为 15m；是根据待配准影像片(d)中白色方框里的区域，通过正反函数表达式和双线性内插公式得到。

2.2 区域自动配准

在区域自动配准法中，考虑到主被动遥感影像传感器不同，时相不同，色调差异较大，本文采用归一化互相关系数法作为相似性测度定义灰度属性。

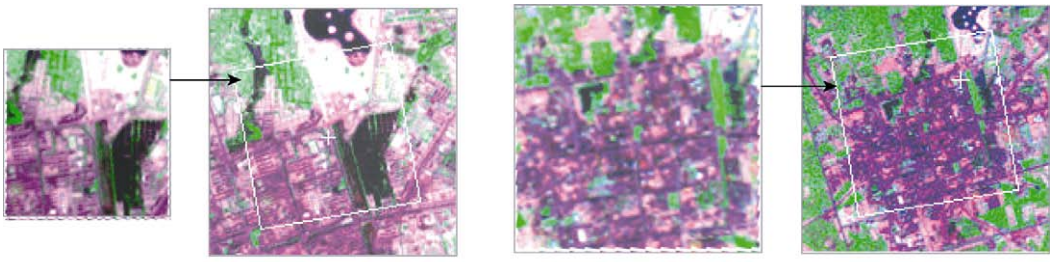

图 2 影像辅助面

(a) 小辅助面, 101×101 像元，分辨率为 15m; (b) 基准影像片，白色方框中的区域为与小辅助面对应的区域，分辨率为 15m; (c) 大辅助面, 201×201 像元，分辨率为 15m; (d) 待配准影像片，白色方框中的区域为与大辅助面对应的区域，分辨率为 30m; (b)和(d)中的十字丝标示的位置，表示同名特征点

归一化互相关系数法是以统计相关原理进行匹配的一种方法，即定义目标窗口和搜索窗口，并让目标窗口在搜索窗口中左右上下逐一移动，移动时将目标窗口与搜索窗口内对应子窗口的灰度值代入目标函数(式(1))，计算互相关系数，互相关系数取得最大值的地方就是最佳的匹配位置，计算公式为:

$$C(u,v)=\frac{\sum_x\sum_y[T(x,y)-\mu_T][I(x-u,y-v)-\mu_{I(u,v)}]}{\sqrt{\sum_x\sum_y[T(x,y)-\mu_T]^2\sum_x\sum_y[I(x,y)-\mu_{I(u,v)}]^2}} \quad (1)$$

式中，$C(u,v)$表示归一化互相关系数，范围为[−1,1]; x, y 表示目标窗口中像元点的行列坐标值; u, v 表示目标窗口相对于搜索窗口的行列偏差值; $T(x,y)$表示目标窗口中像元点的灰度值; $I(x,y)$表示搜索窗口中像元点的灰度值; μ_T 表示目标窗口中所有像元点的灰度均值; $\mu_{I(u,v)}$表示搜索窗口里对应的子窗口中所有像元点的灰度均值。

定义了灰度属性之后，就可以利用 2.1 节中构建的具有相同尺度和角度的大小辅助面组合进行同名点的搜索。定义小辅助面为目标窗口，大辅助面为搜索窗口，采用公式(1)，就可以得到同名特征点在辅助面中的行列坐标值，继而得到对应的地理坐标值。

2.3 正函数变换得到同名点

依据 2.2 节中得到的大小辅助面中同名特征点的地理坐标值，分别采用基准影像和待配准影像的正函数表达式变换，得到基准影像中特征点的行列坐标值和待配准影像中相应特征点的行列坐标值。图 2 (b)(d)中白色十字丝标示的位置表示同名特征点。

2.4 图像配准

由于图像的不同区域在纹理、图像质量等方面存在差异，得到的同名特征点并不都是正确的点，本文对 2.3 节中得到的结果进行统计分析，滤除明显错误的特征点，选取可靠性高的同名特征点组成最佳特征点集，带入最小二乘法(Ackermann, 1983)，求解得到变换模型的参数。变换模型的公式如式(2)。

$$\begin{bmatrix}x'\\y'\end{bmatrix}=\lambda\begin{bmatrix}a_1 & a_2\\b_1 & b_2\end{bmatrix}\begin{bmatrix}x\\y\end{bmatrix}+\begin{bmatrix}\Delta x\\\Delta y\end{bmatrix} \quad (2)$$

式中，λ表示尺度缩放系数；a_i，b_i (i = 1, 2)表示由角度旋转参数的函数组成的方向余弦；$[\Delta x\ \Delta y]^{\mathrm{T}}$ 表示平移参数，$[x\ y]^{\mathrm{T}}$表示待配准影像上的坐标，$[x'\ y']^{\mathrm{T}}$表示配准后的坐标。将式(2)线性化，列出误差方程式和法方程式，求解得到变换模型的参数；然后采用变换模型对待配准图像进行重采样，得出最终配准的结果图。

3 实验与分析

为了验证该算法的可行性，分别选取了被动光学影像中 SPOT 影像和 ASTER 影像组合、主动雷达影像中 ASAR 影像和被动光学影像中 ASTER 影像组合进行了实验。

3.1 SPOT 和 ASTER 的配准实验与分析

采用的配准数据为甘肃省张掖地区的 SPOT 影像和 ASTER 影像(图 3)，其中，SPOT 影像为基准影像，ASTER 影像为待配准影像。设定在基准影像中，沿正北方向上下左右每隔 101 个像元取一个特征点，以该特征点为中心建立一个 101×101 像元的小辅助面，根据原始地理位置偏差设定大辅助面的大小为 201×201 像元。采用结合空间辅助面特征的区域配准法进行配准，共得到 256 对同名特征点，图 4 是所有同名特征点的归一化互相关系数分布图。

由于 SPOT 影像和 ASTER 影像在不同的时间由不同的传感器获取，整体相关系数不高。经过多次实验，发现最小归一化互相关系数的阈值为 0.3，即大于 0.3 才能确保是同名点，而小于 0.3 就可以断定两幅图像在此区域内不存在同名点，选取归一化互相关系数为 0.6 以上的特征点组成最佳特征点集。

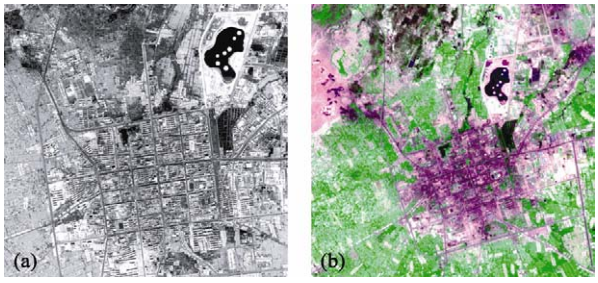

图 3 SPOT 影像和 ASTER 影像配准实验
(甘肃省张掖地区)

(a) SPOT 为影像(全色波段), 2008-03-29 获取，分辨率为 2.5m，角度 0°, 2000×2000 像元，设为基准影像; (b) ASTER 影像(2,3,1 波段合成), 2008-05-23 获取，分辨率为 15m，角度 10.3862°, 500×500 像元，设为待配准影像

根据最佳特征点集，采用最小二乘法求解变换模型参数，运用变换模型对 ASTER 影像进行重采样，如图 5(a)，分辨率和角度与 SPOT 影像相同。为了更好地显示配准的效果，分别提取 SPOT 影像和配准后 ASTER 影像的不同部位相间拼接，形成配准结果图(图 5(b))。通过将图 5 与 ASTER 原始影像(图 3(a))相比，可以看出，各种地物以及纹理在拼接处表现十分平滑和自然，有效地证明了配准结果的精度较高。

3.2 ASAR 影像和 ASTER 影像的配准实验分析

采用的配准数据为北京城区的 ASAR 影像和 ASTER 影像(图 6)，其中，ASAR 影像为基准影像，

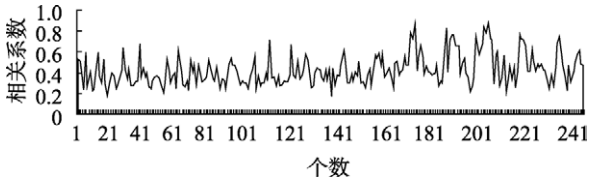

图 4 SPOT 影像和 ASTER 影像的归一化互相关系数分布图

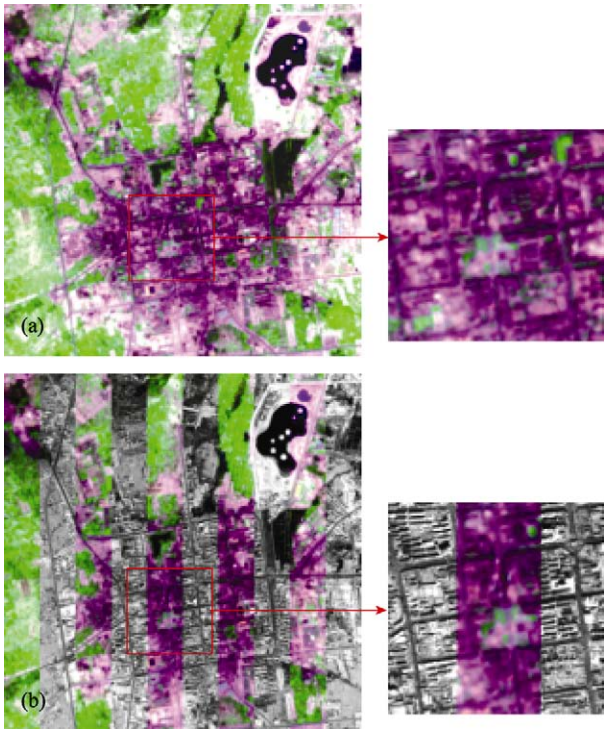

图 5 TM 影像与 ASTER 影像的配准结果图

(a) 配准后的 ASTER 影像，及局部放大图，角度和分辨率等同与 SPOT 影像; (b) 分别提取配准后 ASTER 影像和 SPOT 影像的不同部位相间拼接而成的图像，从左到右，分别是配准后的 ASTER 影像和 SPOT 影像

ASTER 影像为待配准影像。设定在基准影像中，沿着正北方向上下左右每隔 101 个像元取一个特征点，以该特征点为中心建立一个 101×101 像元的小辅助面，根据原始地理位置偏差设定大辅助面的大小为 151×201 像元。采用结合空间辅助面特征的区域配准法进行配准，共得到 81 对同名特征点，图 4 是所有同名特征点的归一化互相关系数分布图。

ASAR 影像是微波图像，记录的是地物的后向散射能；ASTER 影像波段范围为可见光-热红外波段，记录的是地物反射的太阳辐射能或发射的太阳辐射能；两者成像机理不同，配准时整体相关系数偏低。经过多次实验，确定最小归一化互相关系数的阈值为 0.2，选取归一化互相关系数为 0.25 以上的特征点组成最佳特征点集(图 7)。

配准后的 ASTER 影像如图 8(a)；图 8(b)是分别提取 ASAR 影像和配准后 ASTER 图像的不同部位相间拼接形成的结果图像。通过将图 8 与 ASAR 原始影像图 6(a)相比，可以看出，道路、河流、建筑物等地物在拼接处连接自然，纹理平滑，证明了结合空间辅助面特征的区域自动配准法运用在光学图像和雷达图像配准时，可以取得精度较高的结果。

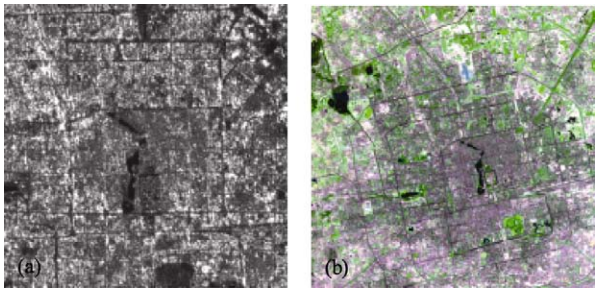

图 6 ASAR 影像和 ASTER 影像配准实验(北京城区)

(a) 为 ASAR 影像(HH 极化方式), 2004-04-27 获取，分辨率为 12.5m，角度 0°, 1000×1000 像元，设为基准影像; (b) ASTER 影像 (2,3,1 波段合成), 2004-04-09 获取，分辨率为 15m，角度 10.3862°, 1500×1500 像元，设为待配准影像

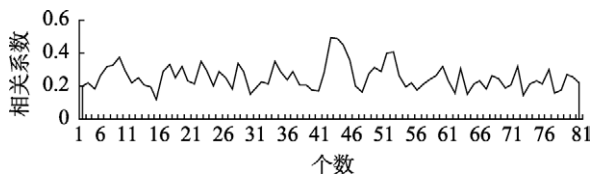

图 7 ASAR 影像和 ASTER 影像的归一化互相关系数分布图

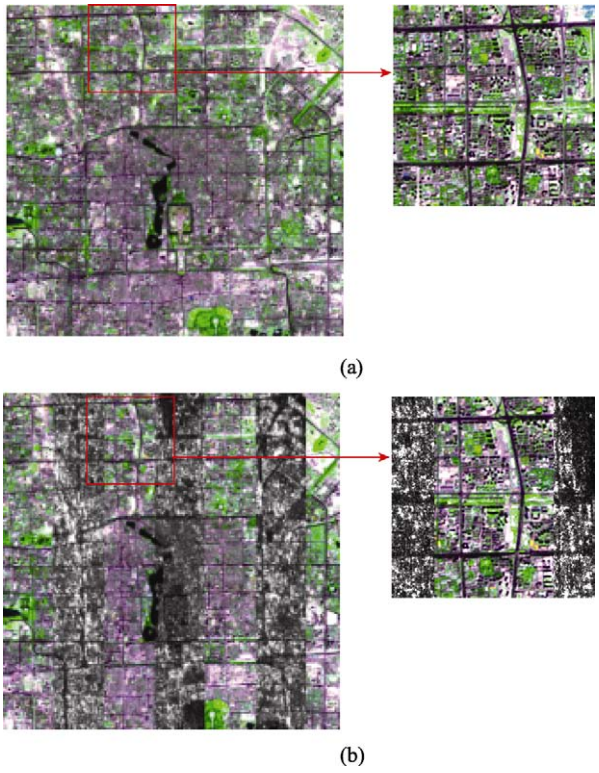

图 8 ASAR 影像与 ASTER 影像的配准结果图

(a) 采用结合空间辅助面特征的区域配准法得到的配准后的 ASTER 影像，角度和分辨率与 ASAR 影像相同; (b) 分别提取配准后 ASTER 影像和 ASAR 影像的不同部位相间拼接而成的图像，从左到右，分别是配准后的 ASTER 影像和 ASAR 影像

4 结 论

本文针对在主被动遥感影像配准中遇到的问题，提出了一种新的基于空间辅助面特征的区域自动配准方法，成功地将空间辅助面特征与灰度属性结合了起来。该算法类似于基于全局区域配准的算法，可以取得较高的精度；但是同名点的搜索不是基于全局区域，而是基于包含具有相同角度和尺度的空间辅助面特征的临时辅助面，有效地降低了算法的计算量和复杂度；同时一定程度上克服了配准影像在尺度和角度上的差异，扩大了算法的适用范围；在区域配准中归一化互相关系数法的采用降低了影像色调差异对配准结果的干扰，提高了算法的鲁棒性。另外，在采用尺度、时相偏差过大的雷达影像和光学影像进行配准时，精度有所下降，进一步研究如何提取针对主被动遥感影像的空间一致性特征是今后工作的重点。

REFERENCES

Ackermann F. 1983. High precision digital image correlation. Proceeding of the 39th Photogrammetric Week

Ardeshir G, George C S and Carl V P. 1986. A region-based approach to digital image registration with subpixel accuracy. *IEEE Transactions on Geoscience and Remote Sensing*, **24**(3): 390—399

Ayaehe N and Fvaerjon B.1985. Fast setero matching of edge segments using prediction and verifi-ceation of hypotheses. Proceedings of Computer Vision and Pattern Cognition

Brown L G. 1992. A survey of image registration techniques. *ACM Computing Survey*, **24**(4): 325—376

Carlotto M J. 1997. Detection and analysis of change in remotely-sensed imagery with application to wide area surveillance. *IEEE Transactions on Image Processing*, **6**(1): 189—202

Chen H, Varshney P and Arora M. 2003. Performance of mutual information similarity measure for registration of multitemporal remote sensing images. *IEEE Transaction on Geoscience and Remote Senseing*, **41**(11): 2445—2454

Förstner W. 1986. A feature based correspondence algorithm for image matching. *International Archives of Photogrammetry and Remote Sensing*, **26**(3): 150—166

Hannah M J. 1989. A system for digital stereo image matching. *Photogrammetric Engineering and Remote Sensing*, **55**(12): 1765—1770

Inglada J. 2002. Similarity measures for multisensor remote sensing images. International Geoscience and Remote Sensing Symposium (IGARSS)

Karna D K, Agarwal S and Nikam S. 2008. Normalized cross-correlation based fingerprint matching. 2008 Fifth International Conference on Computer Graphics, Imaging and Visualisation

Kim T and Im Y. 2003. Automatic satellite image registration by combination of matching and random sample consensus. *IEEE Transaction on Geoscience Remote Sensing*, **41**(5): 1111—1117

Lee H J and Lei W L. 1990. Region matching and depth finding for 3-D objects in stereo aerial photographs. *Pattern Recognition*, **23**(2): 81—93

Maintz J B A and Viergever M A. 1998. A survey of medical image registration. *Medical Image Analysis*, **2**(1): 1—36

Moigne Le, Cole-Rhodes J, Eastman A, Jain R, Joashua P, Memaradeghi A, Mount N, Netanyahu D, Morisette N and Uko-Ozore J. 2006. Image registration and fusion studies for the integration of multiple remote sensing data. International Geoscience and Remote Sensing Symposium 2006 (IGARSS'06)

Shams R, Kennedy R A, Sadeghi P and Hartley R. 2007. Gradient intensity-based registration of multi-modal images of the brain. IEEE 11th International Conference on Computer Vision (ICCV 2007)

Vosselman G. 1992. Relational matching. Springer, Berlin: Lecture Notes in Computer Science

Wen G, Li D and Yuan X. 2002. A global optimal registration method for satellite remote sensing images. Proceedings ISPRS Commission III Symposium

Wen G, Lu J and Yu W. 2008. A high-performance feature-matching method for image registration by combining spatial and similarity information. *IEEE Transactions on Geoscience and Remote Sensing*, **46**(4): 1266—1277

Zhao F, Huang Z and Gao W. 2006. Image matching by normalized cross-correlation. International Conference on Acoustics, Speech and Signal Processing 2006(ICASS'06)